






# Extending the Dark Matter Reach of Water Cherenkov Detectors using Jupiter

Sandra Robles  \*

*Theoretical Particle Physics and Cosmology Group, Department of Physics,  
King's College London, Strand, London, WC2R 2LS, UK  and*

*Particle Theory Department, Theory Division, Fermi National Accelerator Laboratory, Batavia, Illinois 60510, USA *

Stephan A. Meighen-Berger  †

*School of Physics, The University of Melbourne, Victoria 3010, Australia  and  
Center for Cosmology and AstroParticle Physics (CCAPP),  
Ohio State University, Columbus, OH 43210, USA *

(Dated: November 8, 2024)

We propose the first method for water Cherenkov detectors to constrain GeV-scale dark matter (DM) below the solar evaporation mass. While previous efforts have highlighted the Sun and Earth as DM capture targets, we demonstrate that Jupiter is a viable target. Jupiter's unique characteristics, such as its lower core temperature and significant gravitational potential, allow it to capture and retain light DM more effectively than the Sun, particularly in the mass range below 4 GeV where direct detection sensitivity diminishes. Our calculations provide the first bounds on GeV-scale annihilating DM within Jupiter, showing that these bounds surpass current solar limits and direct detection results.

## INTRODUCTION

Over the past years, probing the particle-nature of GeV-scale dark matter (DM), has been believed to be the purview of direct detection experiments [1–11]. These experiments rely on dark matter scattering with nucleons or electrons within the detector, detecting the energy transferred during the interaction.

In recent years, complementary methods via indirect-detection of dark matter have been proposed. If DM does scatter with nucleons or electrons, it can be captured and gravitationally bound within astronomical objects. Already in the 80s, the Sun and Earth were proposed as DM capture targets [12–15]. Soon after, it was realized that accreted DM annihilating or decaying in the center of the Sun or the Earth could give rise to a neutrino signal potentially in the reach of neutrino detectors [16, 17]. By now, this has become a well-established indirect detection technique and many neutrino experiments search for captured (and annihilating) dark matter [18–26]. Indirect searches using the Sun as a target are even able to *outperform* current direct detection results [2, 11]. In particular, this is the case for spin-dependent (SD) DM-nucleon cross-sections, when the captured DM directly annihilates to neutrinos [24, 27]. Such scenarios can be realized in e.g. lepton portal DM models [29, 30].

These indirect DM searches have intrinsic limitations. They require DM to be captured within a given star or planet, settle down in the center of the object via further scatterings and later annihilate. However, *light* DM, can regain energy via collisions within the astrophysical object and escape before annihilating. At which particular mass this starts to happen, depends on the celestial object. Specifically for the Sun, it has been estimated to be

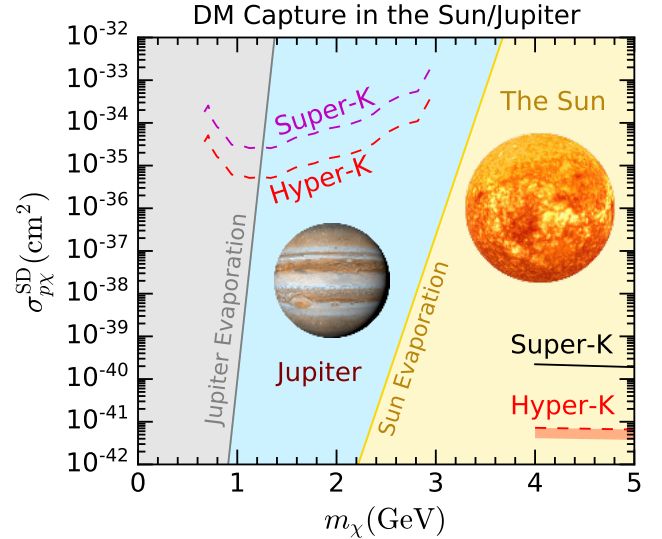


FIG. 1. Sketch of the bounds we set here ( $\nu\bar{\nu}$ ) compared to solar bounds. Super-K  $\tau\tau$ -bounds [19], Hyper-K  $\nu\bar{\nu}$ -estimate [27]. Evaporation mass for the Sun taken from ref. [28]. Using Jupiter, we reach energy regions *inaccessible* to solar searches.

$\sim 4$  GeV [14, 28, 31, 32]. This is a similar mass to where direct detection experiments lose sensitivity.

This leads to *different* astrophysical targets being required to push to lower masses, such as planets. Due to their lower core temperatures, less kinetic energy can be transferred to DM during collisions, reducing the probability of escape. However, a planet's capacity to capture DM is limited having a weaker gravitational potential, which implies they are less efficient at capturing DM

than a star. Balancing these two leads to a narrow mass range, where planets, specifically Jupiter, can capture more light DM than the Sun [33–37].

Here we propose and calculate the first bounds on annihilating DM within Jupiter using existing and future neutrino observatories. We show that this analysis can probe *lighter* masses than current solar bounds and even *exceed* current bounds set by direct detection experiments.

Fig. 1 shows a sketch of the predicted sensitivities and compares them to current and future constraints set using the Sun. *Our primary goal in this paper is to demonstrate searching for Jupiter-bound DM signals in neutrino experiments extends their physics reach and offers complementary results to direct-detection experiments.*

In Section II, we review the physics of neutrino fluxes from captured dark matter. There we show *improved* calculations for DM capture in Jupiter. Then, in Section III, we present our sensitivity predictions for Super-Kamiokande (Super-K) [38], Hyper-Kamiokande (Hyper-K) [39, 40], and ORCA [41]. In Section IV, we conclude. In the Supplemental Material, we provide further information.

## NEUTRINO FLUX FROM DM ANNIHILATION

Jupiter, the largest and oldest planet in the solar system, is a gaseous planet. It is thought to be composed of a two-layer structure envelope enclosing a small rocky core. The envelope is mainly made of hydrogen and helium and also contains small traces of heavier elements. The outer envelope has a lower helium abundance than the inner envelope. Since we consider only DM-nucleon spin dependent interactions, the hydrogen component in the planet’s envelope is the sole target for DM scattering, and elements with no nuclear spin such as helium and heavier elements in the planet’s core do not contribute to any scattering process.

We assume that the DM accumulated in Jupiter annihilates solely to neutrinos with a yield per DM annihilation  $dN_\nu/dE_\nu$ , which in this case is just a delta function at the DM mass energy. The neutrino flux also depends on the DM annihilation rate  $\Gamma_A$  and leads to a flux at a detector on Earth of

$$\frac{d\Phi_\nu}{dE_\nu} = \frac{\Gamma_A}{4\pi D_J^2} \frac{dN_\nu}{dE_\nu}, \quad (1)$$

where  $D_J$  is the Earth-Jupiter distance.

The annihilation rate,  $\Gamma_A = AN_\chi^2/2$ , is determined mainly by the number of particles,  $N_\chi$ , accumulated in Jupiter at the present time and the annihilation cross section through

$$A = \langle \sigma_{\chi\chi} v \rangle \frac{\int n_\chi^2(r) 4\pi r^2 dr}{\left( \int n_\chi(r) 4\pi r^2 \right)^2}, \quad (2)$$

where  $n_\chi$  is the DM number density within Jupiter (see Supplemental Material). Here, we assume a thermal relic, i.e.  $\langle \sigma_{\chi\chi} v \rangle = 3 \times 10^{-26} \text{ cm}^3/\text{s}$  and s-wave annihilation, as done when computing bounds from DM capture in the Sun at neutrino detectors [18–25].

The number of accreted DM particles at a given time, in turn, depends on three competing effects. (i) The rate at which they are captured by Jupiter’s gravitational potential,  $C$ . (ii) Captured DM can scatter again with hydrogen atoms in Jupiter, gain energy and escape the planet before annihilating. This is called evaporation. (iii) The annihilation rate. Both, evaporation and annihilation deplete the number of accumulated DM particles. Then, the number of DM particles is obtained by solving the following differential equation

$$\frac{dN_\chi}{dt} = C - EN_\chi - AN_\chi^2, \quad (3)$$

where  $E$  is the evaporation rate. This equation has an exact analytical solution (see Supplemental Material), provided that capture, annihilation and evaporation rates remain constant throughout most of Jupiter’s lifetime. At present time, the number of DM particles in Jupiter’s core is well approximated by

$$N_\chi \simeq \sqrt{\frac{C}{A}} \frac{1}{\frac{1}{2} E t_{\text{eq}} + \sqrt{1 + \left( \frac{E t_{\text{eq}}}{2} \right)^2}}, \quad (4)$$

where  $t_{\text{eq}} = 1/\sqrt{CA}$  is known as the capture-annihilation timescale. Note that when evaporation is negligible  $N_\chi \simeq \sqrt{C/A}$  and  $\Gamma_A \simeq C/2$ .

The spin-dependent capture rate is proportional to the scattering cross section  $\sigma_{p\chi}^{\text{SD}}$ , which we take to be a constant. To compute capture, evaporation, and annihilation rates in a consistent manner, we use a three-layer model of Jupiter that satisfies observational constraints [42].

In Fig. 2, we show our computation of the capture rate for a DM-proton elastic scattering cross section  $\sigma_{p\chi}^{\text{SD}} = 10^{-35} \text{ cm}^2$  and compare our result in magenta with previous calculations in the literature [34, 43]. The only difference between our calculation and others is that we have made use of a Jupiter model to properly account for the hydrogen number density in Jupiter’s envelope as well as the escape velocity radial profile. The capture rate peaks around the proton mass due to resonance enhancement with hydrogen, as observed in the case of the Earth [14].

To calculate evaporation and annihilation rates we have followed refs. [44, 45]. We used the temperature profile provided by the aforementioned Jupiter model to estimate the DM density and velocity distribution in Jupiter’s core once it has settled down in the center of the planet. Evaporation is relevant for light DM. In the

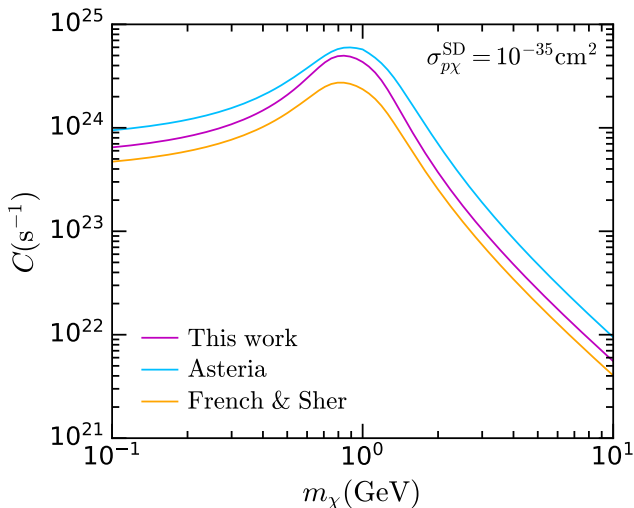


FIG. 2. Spin dependent DM capture rate (magenta) for a DM-proton elastic scattering cross section  $\sigma_{p\chi}^{\text{SD}} = 10^{-35} \text{ cm}^2$ . We also show results obtained with other estimations in the literature [34, 43] for comparison.

particular case of Jupiter, this means DM of mass below  $\sim 1.2 - 1.3 \text{ GeV}$ , relevant for the range of scattering cross sections analyzed here (see Supplemental Material). Below this mass threshold captured DM is expected to evaporate before having the chance to annihilate into neutrinos. The exact value of the evaporation mass, as this threshold is known, can slightly vary around the above-mentioned values for a different assumption of annihilation cross section.

## NEUTRINO EXPERIMENT SENSITIVITIES

To estimate the feasibility of this analysis, we perform a rough estimate of the potential sensitivity: At  $\sigma_{p\chi}^{\text{SD}} = 5 \times 10^{36} \text{ cm}^2$  and  $m_\chi = 1 \text{ GeV}$  the Jupiter capture rate (and annihilation rate) is  $\sim 10^{24} \text{ s}^{-1}$ . Assuming isotropic emission and scaling by the Jupiter-Earth sphere ( $4\pi \times (8 \times 10^{13} \text{ cm})^2$ ), the resulting flux is then  $\sim 10^{-5} (\text{s cm}^2)^{-1}$ . At  $1 \text{ GeV}$  (neutrino energy), the primary background is the atmospheric muon-neutrino flux  $\sim 0.2 (\text{GeV s cm}^2)^{-1}$  [46]. Using an angular resolution of  $2^\circ$  (the sky has  $\sim 40000^\circ$ ) leads to a suppression of the atmospheric flux by  $\sim 10^{-4}$ . This puts the arriving neutrino flux from Jupiter ( $10^{-5} (\text{s cm}^2)^{-1}$ ), on par with the expected atmospheric flux,  $2 \times 10^{-5} (\text{s cm}^2)^{-1}$ . Since we are looking for a neutrino line, this estimate shows that we will search for an excess of events in Jupiter's direction centered at the DM mass.

Currently, the only detector with a significant set of GeV-scale neutrino events is Super-K [38]. In the future JUNO [47], DUNE [48, 49], and Hyper-K [39, 40] will have similar capabilities. Here, we focus on Super-K and

its successor, Hyper-K. Both are cylindrical water-based Cherenkov detectors with fiducial volumes of 22.5 kton and 187 kton, respectively. With excellent energy resolution  $\leq 10\%$  [50–52], angular resolution  $< 2^\circ$  [52], and detection efficiency  $> 80\%$  [53] for CC  $\nu_\mu$  events, these detectors are ideal low-energy point source detectors.

Due to the dark matter evaporation mass  $\sim 1 \text{ GeV}$ , we expect no neutrino signal events below  $100 \text{ MeV}$ . For this reason we restrict our analysis to neutrino energies  $E_\nu \in [100 \text{ MeV}, 5 \text{ GeV}]$ . For these energies, only atmospheric neutrinos will be a significant background. For the neutrino flux above  $100 \text{ MeV}$ , we use HKKM11 [54], which agrees well with Super-K measurements [53].

To predict the number of atmospheric and DM signal events in an energy bin  $j$ , we use

$$\mathcal{N}^j = N_t \Delta t \int_{\omega_j}^{\infty} dE_\nu \frac{d\Phi}{dE_\nu}(E_\nu) \sigma_j(E_\nu), \quad (5)$$

where  $N_t$  is the number of target atoms (oxygen and hydrogen) and  $\Delta t$  is the detector livetime. For the exposure, we assume 15.9 (10) live time years for Super-K (and Hyper-K).  $\sigma$  is the neutrino-oxygen cross section, which get from GENIE 3.2.0 with tune G18.10a.02.11b, which is based on a local Fermi-gas model and an empirical meson-exchange model [55–57].

With 350 (1870) kton-years (15.9 years and 10 years) of Super-K (Hyper-K) data, we predict  $\mathcal{O}(25k)$  ( $\mathcal{O}(100k)$ ) fully contained atmospheric muon neutrino events. These results agree well when scaled to SK data for 1489 days (SK-I), resulting in  $\mathcal{O}(6k)$  events [46, 58].

To reduce this background, we apply angular cuts, defining a region of  $2^\circ$  around the direction of Jupiter and removing all events outside of it. With an angular reconstruction uncertainty of  $\leq 2^\circ$  [52], this removes nearly all of the atmospheric neutrino events, leaving only  $\mathcal{O}(10)$  ( $\mathcal{O}(100)$ ) between  $100 \text{ MeV}$  and  $5 \text{ GeV}$  for Super-K (hyper-K). This makes the search nearly *background-free* for a given energy.

For the sensitivity estimate, we account for a  $\sim 20\%$  uncertainty on the neutrino-oxygen cross section. We then invert the standard frequentist hypothesis test [59] and set lower bounds for different dark matter masses on  $\sigma_{p\chi}^{\text{SD}}$ .

Fig. 3 shows the resulting 95% sensitivities for both Super-K and Hyper-K and compares them to current direct-detection constraints [9]. At  $\sim 1 \text{ GeV}$ , we predict Super-K, with its collected data, can exceed current direct-detection experiments. In the future, these results will then be superseded by Hyper-K due to its larger volume. The sharp cut-off at  $\sim 700 \text{ MeV}$  is caused by the suppression of the capture rate due to evaporation.

We also show a sensitivity prediction for ORCA [41] using the angular resolution from [60] and the effective area from [61]. While ORCA's size means its yield for dark matter masses  $\geq 1.5 \text{ GeV}$  is higher, the larger angular reconstruction error ( $\geq 10^\circ$ ) [62], results in a far

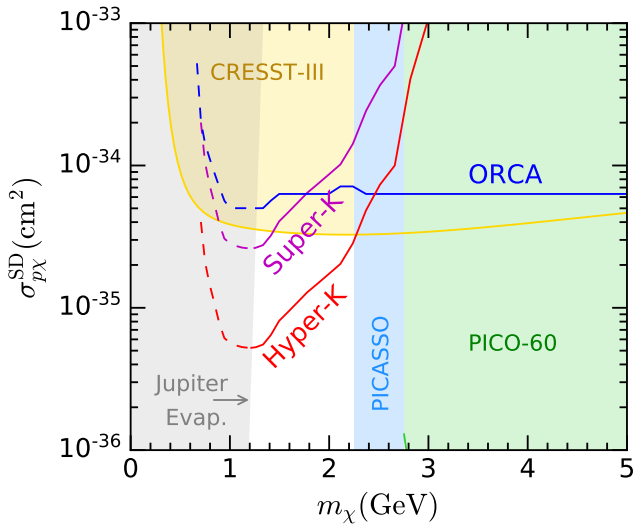


FIG. 3. The 95% sensitivities calculated here for Super-K, Hyper-K, and ORCA. We show the current direct detection constraints by CRESST [9], PICASSO [1] and PICO-60 [2] in green, light blue and yellow, respectively. The gray region shows where evaporation becomes relevant.

larger atmospheric background and a reduction in sensitivity. Improving this would allow ORCA to exceed Hyper-K’s sensitivity.

Here, we exclusively used muon-neutrino events due to the ease of directional reconstruction of muon tracks. These results can easily be improved by including electron neutrino events, doubling the expected signal events.

## CONCLUSION AND DISCUSSION

Currently, the most stringent indirect bounds on GeV scale DM scattering off protons are set by observing the Sun. The reach of this method is naturally limited by the DM evaporation mass of the Sun.

Here, we proposed a new method to push these bounds to even lower DM masses by searching for neutrinos in the direction of Jupiter. These neutrinos are produced by captured DM annihilating within Jupiter. While the expected signal flux lies far below the atmospheric neutrino flux, Super-K’s and Hyper-K’s excellent angular reconstruction can suppress the atmospheric neutrino flux to such an extent that this new signal will appear as an *excess* in neutrino events in the direction of Jupiter.

Using exclusively muon-neutrino events, we showed that Super-K can *exceed* current direct detection constraints for dark matter interactions at approximately 1 GeV, while Hyper-K can improve on them even further. In the future, these bounds can be further improved by including electron-neutrino events. While the directional reconstruction is slightly worse [52], the expected background is reduced [54], making this channel potentially

better than the one chosen here.

## ACKNOWLEDGMENTS

SR was partially supported by the UK STFC grant ST/T000759/1 and by the Fermi National Accelerator Laboratory (Fermilab), a U.S. Department of Energy, Office of Science, HEP User Facility. This work was performed in part at Aspen Center for Physics, which is supported by National Science Foundation grant PHY-2210452. SR acknowledges CERN TH Department for its hospitality while this research was being carried out. SMB was supported by the Australian Research Council through Discovery Project DP220101727 plus the University of Melbourne’s Research Computing Services and the Petascale Campus Initiative.

\* sroble@fnal.gov

† stephan.meighenberger@unimelb.edu.au

- [1] E. Behnke *et al.*, Final Results of the PICASSO Dark Matter Search Experiment, *Astropart. Phys.* **90**, 85 (2017), arXiv:1611.01499 [hep-ex].
- [2] C. Amole *et al.* (PICO), Dark Matter Search Results from the Complete Exposure of the PICO-60 C<sub>3</sub>F<sub>8</sub> Bubble Chamber, *Phys. Rev. D* **100**, 022001 (2019), arXiv:1902.04031 [astro-ph.CO].
- [3] E. Aprile *et al.* (XENON), Light Dark Matter Search with Ionization Signals in XENON1T, *Phys. Rev. Lett.* **123**, 251801 (2019), arXiv:1907.11485 [hep-ex].
- [4] E. Aprile *et al.* (XENON), Search for Light Dark Matter Interactions Enhanced by the Migdal Effect or Bremsstrahlung in XENON1T, *Phys. Rev. Lett.* **123**, 241803 (2019), arXiv:1907.12771 [hep-ex].
- [5] E. Aprile *et al.* (XENON), Search for Coherent Elastic Scattering of Solar <sup>8</sup>B Neutrinos in the XENON1T Dark Matter Experiment, *Phys. Rev. Lett.* **126**, 091301 (2021), arXiv:2012.02846 [hep-ex].
- [6] C. Fu *et al.* (PandaX-II), Spin-Dependent Weakly-Interacting-Massive-Particle–Nucleon Cross Section Limits from First Data of PandaX-II Experiment, *Phys. Rev. Lett.* **118**, 071301 (2017), [Erratum: Phys.Rev.Lett. 120, 049902 (2018)].
- [7] Y. Meng *et al.* (PandaX-4T), Dark Matter Search Results from the PandaX-4T Commissioning Run, *Phys. Rev. Lett.* **127**, 261802 (2021), arXiv:2107.13438 [hep-ex].
- [8] J. Aalbers *et al.* (LUX-ZEPLIN), First Dark Matter Search Results from the LUX-ZEPLIN (LZ) Experiment, *Phys. Rev. Lett.* **131**, 041002 (2023), arXiv:2207.03764 [hep-ex].
- [9] G. Angloher *et al.* (CRESST), Testing spin-dependent dark matter interactions with lithium aluminate targets in CRESST-III, *Phys. Rev. D* **106**, 092008 (2022), arXiv:2207.07640 [astro-ph.CO].
- [10] D. H. Lee *et al.*, COSINE-100U: Upgrading the COSINE-100 Experiment for Enhanced Sensitivity to Low-Mass Dark Matter Detection (2024) arXiv:2409.15748 [hep-ex].



- [11] J. Aalbers *et al.* (LZ Collaboration), Dark Matter Search Results from 4.2 Tonne-Years of Exposure of the LUX-ZEPLIN (LZ) Experiment (2024) [arXiv:2410.17036 \[hep-ex\]](#).
- [12] D. N. Spergel and W. H. Press, Effect of hypothetical, weakly interacting, massive particles on energy transport in the solar interior, *Astrophys. J.* **294**, 663 (1985).
- [13] W. H. Press and D. N. Spergel, Capture by the sun of a galactic population of weakly interacting, massive particles, *Astrophys. J.* **296**, 679 (1985).
- [14] A. Gould, Resonant Enhancements in Weakly Interacting Massive Particle Capture by the Earth, *Astrophys. J.* **321**, 571 (1987).
- [15] A. Gould, Weakly Interacting Massive Particle Distribution in and Evaporation from the Sun, *Astrophys. J.* **321**, 560 (1987).
- [16] J. Faulkner and R. L. Gilliland, Weakly interacting, massive particles and the solar neutrino flux, *Astrophys. J.* **299**, 994 (1985).
- [17] J. Silk, K. A. Olive, and M. Srednicki, The Photino, the Sun and High-Energy Neutrinos, *Phys. Rev. Lett.* **55**, 257 (1985).
- [18] T. Tanaka *et al.* (Super-Kamiokande), An Indirect Search for WIMPs in the Sun using 3109.6 days of upward-going muons in Super-Kamiokande, *Astrophys. J.* **742**, 78 (2011), [arXiv:1108.3384 \[astro-ph.HE\]](#).
- [19] K. Choi *et al.* (Super-Kamiokande), Search for neutrinos from annihilation of captured low-mass dark matter particles in the Sun by Super-Kamiokande, *Phys. Rev. Lett.* **114**, 141301 (2015), [arXiv:1503.04858 \[hep-ex\]](#).
- [20] S. Adrian-Martinez *et al.* (ANTARES), Limits on Dark Matter Annihilation in the Sun using the ANTARES Neutrino Telescope, *Phys. Lett. B* **759**, 69 (2016), [arXiv:1603.02228 \[astro-ph.HE\]](#).
- [21] M. G. Aartsen *et al.* (IceCube), Search for annihilating dark matter in the Sun with 3 years of IceCube data, *Eur. Phys. J. C* **77**, 146 (2017), [Erratum: *Eur. Phys. J. C* **79**, no.3, 214 (2019)], [arXiv:1612.05949 \[astro-ph.HE\]](#).
- [22] M. G. Aartsen *et al.* (IceCube), Search for annihilating dark matter in the Sun with 3 years of IceCube data, *Eur. Phys. J. C* **77**, 146 (2017), [Erratum: *Eur. Phys. J. C* **79**, 214 (2019)], [arXiv:1612.05949 \[astro-ph.HE\]](#).
- [23] S. Adrian-Martinez *et al.* (ANTARES), Limits on Dark Matter Annihilation in the Sun using the ANTARES Neutrino Telescope, *Phys. Lett. B* **759**, 69 (2016), [arXiv:1603.02228 \[astro-ph.HE\]](#).
- [24] R. Abbasi *et al.* (IceCube), Search for GeV-scale dark matter annihilation in the Sun with IceCube DeepCore, *Phys. Rev. D* **105**, 062004 (2022), [arXiv:2111.09970 \[astro-ph.HE\]](#).
- [25] A. Gupta, D. Majumdar, and A. Halder, KM3NeT upper bounds of detection rates of solar neutrinos from annihilations of dark matter at the solar core, *Mod. Phys. Lett. A* **37**, 2250233 (2022), [arXiv:2203.13697 \[hep-ph\]](#).
- [26] G. Renzi and J. A. Aguilar (IceCube), Search for dark matter annihilations in the center of the Earth with IceCube, in *38th International Cosmic Ray Conference* (2023) [arXiv:2308.02920 \[astro-ph.HE\]](#).
- [27] N. F. Bell, M. J. Dolan, and S. Robles, Searching for dark matter in the Sun using Hyper-Kamiokande, *JCAP* **11** (2021), 004, [arXiv:2107.04216 \[hep-ph\]](#).
- [28] G. Busoni, A. De Simone, and W.-C. Huang, On the Minimum Dark Matter Mass Testable by Neutrinos from the Sun, *JCAP* **07** (2013), 010, [arXiv:1305.1817 \[hep-ph\]](#).
- [29] S. Okawa and Y. Omura, Light mass window of lepton portal dark matter, *JHEP* **02** (2021), 231, [arXiv:2011.04788 \[hep-ph\]](#).
- [30] S. Iguro, S. Okawa, and Y. Omura, Light lepton portal dark matter meets the LHC, *JHEP* **03** (2023), 010, [arXiv:2208.05487 \[hep-ph\]](#).
- [31] K. Griest and D. Seckel, Cosmic Asymmetry, Neutrinos and the Sun, *Nucl. Phys. B* **283**, 681 (1987), [Erratum: *Nucl. Phys. B* **296**, 1034–1036 (1988)].
- [32] D. Hooper, F. Petriello, K. M. Zurek, and M. Kamionkowski, The New DAMA Dark-Matter Window and Energetic-Neutrino Searches, *Phys. Rev. D* **79**, 015010 (2009), [arXiv:0808.2464 \[hep-ph\]](#).
- [33] R. K. Leane and T. Linden, First Analysis of Jupiter in Gamma Rays and a New Search for Dark Matter, *Phys. Rev. Lett.* **131**, 071001 (2023), [arXiv:2104.02068 \[astro-ph.HE\]](#).
- [34] G. M. French and M. Sher, Monoenergetic neutrinos from WIMP annihilation in Jupiter, *Phys. Rev. D* **106**, 115037 (2022), [arXiv:2210.04761 \[hep-ph\]](#).
- [35] C. Blanco and R. K. Leane, Search for Dark Matter Ionization on the Night Side of Jupiter with Cassini, *Phys. Rev. Lett.* **132**, 261002 (2024), [arXiv:2312.06758 \[hep-ph\]](#).
- [36] S. Ansarifard and Y. Farzan, Jovian signal at BOREXINO, *Phys. Rev. D* **110**, 063002 (2024), [arXiv:2401.13043 \[hep-ph\]](#).
- [37] C. Blanco, R. K. Leane, M. Moore, and J. Tong, Search for Dark Matter Induced Airglow in Planetary Atmospheres (2024) [arXiv:2408.15318 \[hep-ph\]](#).
- [38] Y. Fukuda *et al.* (Super-Kamiokande), The Super-Kamiokande detector, *Nucl. Instrum. Meth. A* **501**, 418 (2003).
- [39] K. Abe *et al.* (Hyper-Kamiokande), Hyper-Kamiokande Design Report, (2018), [arXiv:1805.04163 \[physics.ins-det\]](#).
- [40] J. Bian *et al.* (Hyper-Kamiokande), Hyper-Kamiokande Experiment: A Snowmass White Paper, in *Snowmass 2021* (2022) [arXiv:2203.02029 \[hep-ex\]](#).
- [41] S. Adrian-Martinez *et al.* (KM3Net), Letter of intent for KM3NeT 2.0, *J. Phys. G* **43**, 084001 (2016), [arXiv:1601.07459 \[astro-ph.IM\]](#).
- [42] N. Nettelmann, A. Becker, B. Holst, and R. Redmer, Jupiter Models with Improved Ab Initio Hydrogen Equation of State (H-REOS.2), *Astrophys. J.* **750**, 52 (2012), [arXiv:1109.5644 \[astro-ph.EP\]](#).
- [43] R. K. Leane and J. Smirnov, Dark matter capture in celestial objects: treatment across kinematic and interaction regimes, *JCAP* **12** (2023), 040, [arXiv:2309.00669 \[hep-ph\]](#).
- [44] R. Garani and S. Palomares-Ruiz, Dark matter in the Sun: scattering off electrons vs nucleons, *JCAP* **05** (2017), 007, [arXiv:1702.02768 \[hep-ph\]](#).
- [45] G. Busoni, A. De Simone, P. Scott, and A. C. Vincent, Evaporation and scattering of momentum- and velocity-dependent dark matter in the Sun, *JCAP* **10** (2017), 037, [arXiv:1703.07784 \[hep-ph\]](#).
- [46] B. Zhou and J. F. Beacom, First detailed calculation of atmospheric neutrino foregrounds to the diffuse supernova neutrino background in Super-Kamiokande, *Phys. Rev. D* **109**, 103003 (2024), [arXiv:2311.05675 \[hep-ph\]](#).
- [47] A. Abusleme *et al.* (JUNO), JUNO physics and detector, *Prog. Part. Nucl. Phys.* **123**, 103927 (2022), [arXiv:2104.02565 \[hep-ex\]](#).

- [48] R. Acciarri *et al.* (DUNE), Long-Baseline Neutrino Facility (LBNF) and Deep Underground Neutrino Experiment (DUNE): Conceptual Design Report, Volume 2: The Physics Program for DUNE at LBNF, (2015), [arXiv:1512.06148 \[physics.ins-det\]](#).
- [49] B. Abi *et al.* (DUNE), Deep Underground Neutrino Experiment (DUNE), Far Detector Technical Design Report, Volume II: DUNE Physics, (2020), [arXiv:2002.03005 \[hep-ex\]](#).
- [50] M. Shiozawa (Super-Kamiokande), Reconstruction algorithms in the Super-Kamiokande large water Cherenkov detector, *Nucl. Instrum. Meth. A* **433**, 240 (1999).
- [51] E. Drakopoulou, G. A. Cowan, M. D. Needham, S. Playfer, and M. Taani, Application of machine learning techniques to lepton energy reconstruction in water Cherenkov detectors, *JINST* **13** (04), P04009, [arXiv:1710.05668 \[physics.ins-det\]](#).
- [52] M. Jiang *et al.* (Super-Kamiokande), Atmospheric Neutrino Oscillation Analysis with Improved Event Reconstruction in Super-Kamiokande IV, *PTEP* **2019**, 053F01 (2019), [arXiv:1901.03230 \[hep-ex\]](#).
- [53] E. Richard *et al.* (Super-Kamiokande), Measurements of the atmospheric neutrino flux by Super-Kamiokande: energy spectra, geomagnetic effects, and solar modulation, *Phys. Rev. D* **94**, 052001 (2016), [arXiv:1510.08127 \[hep-ex\]](#).
- [54] M. Honda, T. Kajita, K. Kasahara, and S. Midorikawa, Improvement of low energy atmospheric neutrino flux calculation using the JAM nuclear interaction model, *Phys. Rev. D* **83**, 123001 (2011), [arXiv:1102.2688 \[astro-ph.HE\]](#).
- [55] C. Andreopoulos *et al.*, The GENIE Neutrino Monte Carlo Generator, *Nucl. Instrum. Meth. A* **614**, 87 (2010), [arXiv:0905.2517 \[hep-ph\]](#).
- [56] C. Andreopoulos, C. Barry, S. Dytman, H. Gallagher, T. Golan, R. Hatcher, G. Perdue, and J. Yarba, The GENIE Neutrino Monte Carlo Generator: Physics and User Manual, (2015), [arXiv:1510.05494 \[hep-ph\]](#).
- [57] J. Tena-Vidal *et al.* (GENIE), Neutrino-nucleon cross-section model tuning in GENIE v3, *Phys. Rev. D* **104**, 072009 (2021), [arXiv:2104.09179 \[hep-ph\]](#).
- [58] Y. Ashie *et al.* (Super-Kamiokande), A Measurement of atmospheric neutrino oscillation parameters by SUPER-KAMIOKANDE I, *Phys. Rev. D* **71**, 112005 (2005), [arXiv:hep-ex/0501064](#).
- [59] G. J. Feldman and R. D. Cousins, A Unified approach to the classical statistical analysis of small signals, *Phys. Rev. D* **57**, 3873 (1998), [arXiv:physics/9711021](#).
- [60] S. Aiello *et al.* (KM3NeT), Event reconstruction for KM3NeT/ORCA using convolutional neural networks, *JINST* **15** (10), P10005, [arXiv:2004.08254 \[astro-ph.IM\]](#).
- [61] F. Benfenati, F. Filippini, and T. Chiarusi (KM3NeT), First scientific results of the KM3NeT neutrino telescope, *EPJ Web Conf.* **283**, 04009 (2023).
- [62] S. Galatà (KM3NeT), Reconstruction of track-type neutrino events in KM3NeT/ORCA, *PoS ICRC2015*, 1102 (2016).
- [63] A. Gould, Big Bang Archeology: WIMP Capture by the Earth at Finite Optical Depth, *Astrophys. J.* **387**, 21 (1992).
- [64] H. Hong and A. C. Vincent, Dark matter limits from the tip of the red giant branch of globular clusters, (2024), [arXiv:2407.08773 \[hep-ph\]](#).
- [65] A. Gould, Evaporation of WIMPs with Arbitrary Cross Sections, *Astrophys. J.* **356**, 302 (1990).
- [66] A. Bottino, G. Fiorentini, N. Fornengo, B. Ricci, S. Scopel, and F. L. Villante, Does solar physics provide constraints to weakly interacting massive particles?, *Phys. Rev. D* **66**, 053005 (2002), [arXiv:hep-ph/0206211](#).
- [67] P. Scott, M. Fairbairn, and J. Edsjo, Dark stars at the Galactic centre - the main sequence, *Mon. Not. Roy. Astron. Soc.* **394**, 82 (2009), [arXiv:0809.1871 \[astro-ph\]](#).
- [68] H. Banks, S. Ansari, A. C. Vincent, and P. Scott, Simulation of energy transport by dark matter scattering in stars, *JCAP* **04** (2022), 002, [arXiv:2111.06895 \[hep-ph\]](#).

## SUPPLEMENTAL MATERIAL

Here, we provide additional details that may be helpful. We discuss capture rate calculations, evaporation rates, annihilation rates, and flux comparisons.

### Capture rate

The DM capture rate in the Earth was first calculated by Gould [14]. A similar approach can be adopted for Jupiter, i.e.

$$C = 4\pi \frac{\rho_\chi}{m_\chi} \int_0^{R_J} dr r^2 \int_0^\infty du_\chi \frac{w(r)}{u_\chi} f_{\text{MB}}(u_\chi) \Omega^-(w), \quad (6)$$

where  $f_{\text{MB}}(u_\chi)$  is the DM velocity distribution far from the Solar system, that we have taken to be Maxwell-Boltzmann (MB) and defined as in ref. [45],  $w(r) = \sqrt{u_\chi^2 + v_{\text{esc}}^2(r)}$  is the DM speed at a radial distance  $r$  from the planet before the collision takes place, and  $v_{\text{esc}}$  is the escape velocity. To calculate the scattering rate  $\Omega^-$ , we consider spin-dependent interactions parameterized by a constant DM-proton cross section  $\sigma_{p\chi}^{\text{SD}}$ . This is the only available targets are hydrogen atoms. In addition, in the DM mass regime we are interested in, we can safely neglect the thermal motion of the targets, whose temperature can reach at most  $\mathcal{O}(1\text{eV})$  in the center of the planet [42]. Thus, the DM scattering rate from a velocity  $w(r)$  to a velocity lower than the escape velocity is given by [45]

$$\Omega^-(w) = \frac{\mu_+^2}{\mu w} \sigma_{p\chi}^{\text{SD}} n_H(r) \left( v_{\text{esc}}^2(r) - w^2 \frac{\mu_-^2}{\mu_+^2} \right) \Theta \left( v_{\text{esc}}^2(r) - w^2 \frac{\mu_-^2}{\mu_+^2} \right),$$

where  $\mu = m_\chi/m_H$ ,  $\mu_\pm = (\mu \pm 1)/2$  and  $n_H(r)$  is the hydrogen number density.

From Eqs. 6 and 7, the capture rate scales linearly with  $\sigma_{p\chi}^{\text{SD}}$ . However, if the cross section is larger than a certain threshold value, the capture rate will begin to saturate to its maximum value, the so-called geometric limit. In this limit all DM particles traversing the planet are captured regardless of the value of  $\sigma_{p\chi}^{\text{SD}}$ . To account for this, we introduce an optical factor  $\eta(r)$  in Eq. 6, whose purpose is to remove captured DM particles from the incoming DM flux, and is in principle a function of the optical depth  $\tau_\chi$  seen by a DM particle as it goes through the planet's envelope [63]

$$\eta(\tau_\chi) = e^{-\tau_\chi}. \quad (7)$$

To calculate the optical depth at a specific radial position we use the approach of refs. [45, 63, 64]. It is noteworthy that ref. [34] assumed the geometric cross section to be  $10^{-34} \text{cm}^2$  for the same DM mass range we have considered, while we find it varies in the range  $\sim 3 \times 10^{-33} - 10^{-31} \text{cm}^2$ .

### Evaporation rate

As the capture process, the evaporation rate has also been previously studied, initially in the context of the Sun [15, 44, 45, 65], which is the relevant regime for Jupiter

$$E = \int_0^{R_J} dr 4\pi r^2 \eta(r) n_\chi(r) \int_0^{v_{\text{esc}}(r)} dw 4\pi w^2 f_\chi(w, r) \Omega^+(w), \quad (8)$$

where  $n_\chi$  and  $f_\chi$  are the DM number density and velocity distribution within Jupiter, respectively. We calculate the latter using an interpolation between the isothermal (iso) and local thermodynamical equilibrium (LTE) regimes [44, 45, 66–68], i.e.

$$n_\chi(r) f_\chi(w, r) = [1 - f(K)] n_\chi^{\text{iso}}(r) \left( \frac{m_\chi}{2\pi T_\chi} \right)^{3/2} \exp \left[ -\frac{m_\chi w^2}{2T_\chi} \right] + f(K) n_\chi^{\text{LTE}}(r) \left( \frac{m_\chi}{2\pi T_J(r)} \right)^{3/2} \exp \left[ -\frac{m_\chi w^2}{2T_J(r)} \right]. \quad (9)$$

where  $T_\chi$  is the temperature of the DM isothermal distribution as defined in ref. [45],  $T_J(r)$  is Jupiter's temperature at a given radial shell  $r$ , and

$$f(K) \approx \frac{1}{1 + (K/K_0)^{1/\tau}}, \quad (10)$$

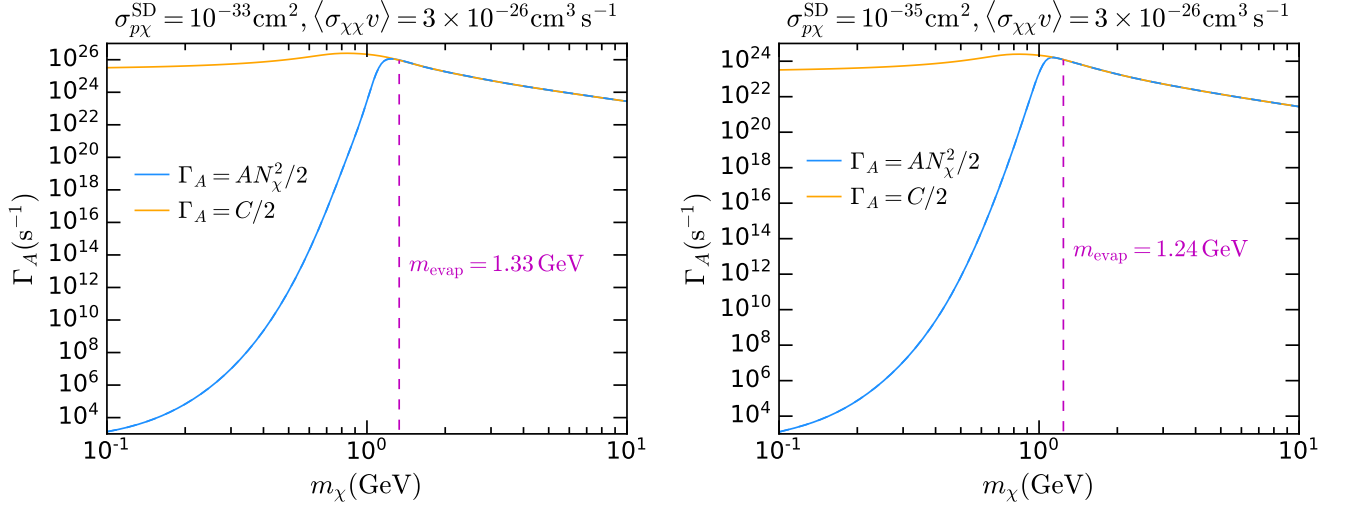


FIG. 4. Illustration of the calculation of the evaporation mass. The exact computation of the annihilation rate is shown in blue, and the corresponding approximation when evaporation is negligible is depicted in orange. The evaporation mass for different values of  $\sigma_{p\chi}^{\text{SD}}$  is shown in magenta.

where  $K_0 = 0.4$  and  $\tau = 0.5$  for the Sun [66, 67].  $K$  is the Knudsen number calculated as the ratio of the mean free path  $\ell = 1/(n_H \sigma_{p\chi})$  to the radius of the DM virialized distribution  $r_\chi$

$$K = \frac{\ell}{r_\chi}, \quad r_\chi = \sqrt{\frac{3T_J(0)}{2\pi G \rho_c m_\chi}}, \quad (11)$$

with  $\rho_c$  the density at Jupiter's center. The expressions for  $n_\chi^{\text{iso}}$  (large mean free path) and  $n_\chi^{\text{LTE}}$  (short mean free path) can be found in refs. [44, 45].

Finally, the up-scattering rate  $\Omega^+$ , which is the probability of captured DM to gain energy in subsequent collisions and achieve a velocity greater than the escape velocity, reads

$$\Omega^+(w) = \frac{16\mu_+^4}{\sqrt{\pi}} \sigma_{p\chi}^{\text{SD}} \int_{v_{\text{esc}}(r)}^\infty dv \int_0^\infty ds \int_0^\infty dt' \left[ \frac{m_p}{2T_J(r)} \right]^{3/2} n_H(r) \frac{vt'}{w} \exp \left[ -\frac{m_p}{2T_J(r)} v_T^2 \right] \Theta(t' + s - v) \Theta(w - |t' - s|), \quad (12)$$

where  $v_T^2 = 2\mu\mu_+(t')^2 + 2\mu_+s^2 - \mu w^2$  is the target squared velocity before the collision in the center of mass (CoM),  $s$  is the CoM velocity, and  $t'$  the DM initial speed also in the CoM frame.

### Annihilation rate

To calculate the annihilation rate, specifically the factor  $A$ , we have assumed s-wave annihilation [28, 44], which leads to

$$A = \langle \sigma_{\chi\chi} v \rangle \frac{\int n_\chi^2(r) 4\pi r^2 dr}{\left( \int n_\chi(r) 4\pi r^2 \right)^2}, \quad (13)$$

with the DM number density in Jupiter calculated again using the fit  $f(K)$

$$n_\chi(r) = [1 - f(K)] n_\chi^{\text{iso}}(r) + f(K) n_\chi^{\text{LTE}}(r). \quad (14)$$

For completeness, we give here the exact solution to the equation for the number of DM particles in Jupiter, Eq. 3

$$N_\chi(t) = \sqrt{\frac{C}{A}} \left[ \frac{\tanh(\beta t/t_{\text{eq}})}{\beta + \frac{1}{2} E t_{\text{eq}} \tanh(\beta t/t_{\text{eq}})} \right], \quad (15)$$



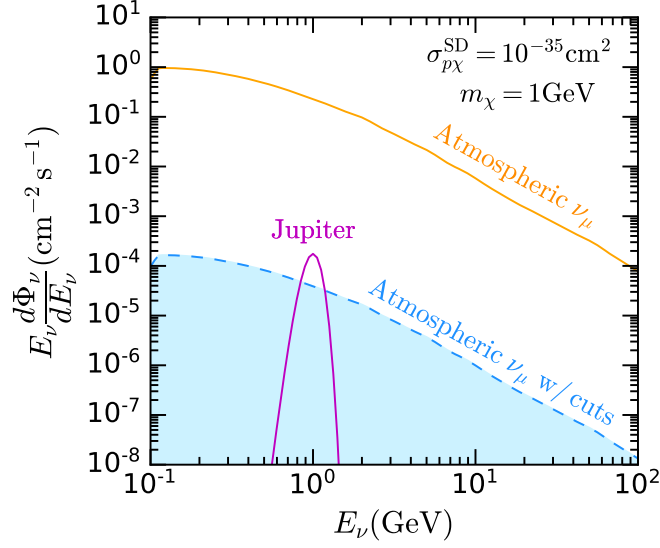


FIG. 5. A comparison of the atmospheric muon neutrino flux at Kamioka [54] (orange) and the expected flux from DM annihilation (magenta). The dashed blue line shows the expected flux after directional cuts.

where

$$\beta = \sqrt{1 + \left(\frac{E t_{\text{eq}}}{2}\right)^2}. \quad (16)$$

Note that when  $\beta t \gg t_{\text{eq}}$ , we obtain the approximation given in Eq. 4.

Finally, once we have calculated capture, evaporation and annihilation rates, we can estimate the evaporation mass  $m_{\text{evap}}$ . This is done by requiring the approximation of the annihilation when evaporation is negligible  $\Gamma_A = C/2$  to be 99% of the exact expression  $\Gamma_A = AN_\chi^2/2$ , with  $N_\chi$  given by Eq. 15 and  $t = 3.4 \text{ Gyr}$ , a Gyr less than the actual Jupiter's age [42] to account for any possible change in the planet's structure, composition and temperature that could lead to different values of the capture, evaporation and annihilation rates. We showcase this estimation in Fig. 4. It is evident that we cannot use the approximation  $\Gamma_A = C/2$ , for DM masses below  $m_{\text{evap}}$ , i.e. the sub-GeV regime, since evaporation makes the annihilation rate dramatically be suppressed by several orders of magnitude.

### Signal and background flux comparison

In Fig. 5, we compare the arriving muon neutrino flux from Jupiter due to DM annihilation and the atmospheric background flux [54] before and after directional cuts. The angular cuts cause a reduction of  $\sim 10000$ . This causes the expected flux from Jupiter at  $\sigma_{p\chi}^{\text{SD}} = 10^{-35} \text{ cm}^2$  to *exceed* the expected background. For the fluxes shown, we have included a 10% energy smearing.